ISSN 2963-7511
Journal of Engineering Researcher and Lecturer, Vol. 5, No. 2, 2026, pp. 81-94

Post-weld heat treatment of GTAW-repaired aluminium 6061-T6 calliper brackets: Effects on surface integrity and micro vickers hardness

Dipo Ariyo Nugroho*, Zainal Abadi, Rifelino, Andril Arafat

Department Mechanical Engineering, Faculty of Engineering, Universitas Negeri Padang, **Indonesia**

*Corresponding Author: dipoariyonugroho03@gmail.com

Received: 23 March 2026; *Revised*: 15 May 2026; *Accepted*: 02 June 2026

https://doi.org/10.58712/jerel.v5i2.218

Abstract: The caliper bracket is a critical component of a motorcycle braking system that maintains the alignment between the brake caliper and the rotor. Repair of damaged caliper brackets is commonly carried out using the Gas Tungsten Arc Welding (GTAW) process. However, the thermal cycle during welding may alter the microstructure and degrade the mechanical properties of Aluminum 6061-T6. To overcome this limitation, post-weld heat treatment (PWHT), in accordance with ASTM B918, can be applied to restore the material properties and enhance the quality of the welded joint. This study investigates the effect of PWHT on the surface quality and microhardness of Aluminum 6061-T6 caliper brackets repaired using the GTAW process. An experimental approach was employed in which all specimens were welded using identical welding parameters and subsequently subjected to PWHT consisting of solution heat treatment, quenching, and artificial aging. Surface quality was evaluated through liquid penetrant testing in accordance with ASTM E165, while microhardness was measured using the Micro Vickers hardness test based on ASTM E384. The penetrant test results revealed that the welded specimens before PWHT contained welding defects, including porosity, lack of fusion, and lack of penetration, with a total of 35 defect indications. After PWHT, the number of defect indications decreased to 19, consisting only of microscopic porosity and lack of fusion. The average microhardness increased from 67.34 HV to 92.26 HV in the Fusion Zone (FZ), from 69.66 HV to 97.78 HV in the Heat-Affected Zone (HAZ), and from 62.44 HV to 95.70 HV in the Base Metal (BM), corresponding to increases of 45.66%, 40.49%, and 53.27%, respectively. Furthermore, PWHT restored the material hardness to 91.62% of the raw material hardness (103.96 HV). These findings demonstrate that PWHT effectively improves both the mechanical performance and the overall quality of GTAW-repaired Aluminum 6061-T6 caliper brackets.

Keywords: Aluminium 6061-T6; Calliper Bracket; GTAW; Micro Vickers Hardness; Penetrant Testing; Post-Weld Heat Treatment

1. Introduction

The advancement of the automotive industry has driven the increasing use of materials with a high strength-to-weight ratio. One of the most widely used materials is Aluminium 6061-T6 due to its excellent combination of mechanical properties, high corrosion resistance, and ease of manufacturing (Rajakumar et al., 2011). This alloy is strengthened by Mg_2Si precipitates, which play a crucial role in enhancing the strength and hardness of the material (Kumar et al., 2019). With an ultimate tensile strength of up to 310 MPa and a yield strength of 276 MPa, Aluminum 6061-T6 is widely used in structural automotive components, such as calliper brackets (Liu et al., 2026).

The calliper bracket is a critical component of the disc brake system that supports the brake calliper and maintains its alignment with the rotor, thereby ensuring optimal braking performance. During

vehicle operation, this component is subjected to a combination of shear force, compressive force, bending moment, and braking torque under repeated loading conditions (Croccolo et al., 2013). In addition, external factors such as impacts and traffic accidents may cause damage in the form of cracks or fractures, potentially reducing the effectiveness and safety of the braking system (Shukla & Choudhary, 2022). Field observations indicate that damage to calliper brackets is still encountered in some vehicles and is commonly repaired by welding because it is more economical than replacing the component with a new one.

One of the most widely used welding methods for repairing aluminium components is Gas Tungsten Arc Welding (GTAW) (Stewart, 2021). This process is capable of producing high-quality welded joints with excellent arc stability and minimal contamination (Carvalho et al., 2024). However, the thermal cycle during welding can alter the microstructure, dissolve strengthening precipitates, and eliminate the T6 temper condition in the Fusion Zone (FZ) and the Heat-Affected Zone (HAZ) (Cheng et al., 2021; Z. Wang et al., 2023, 2024). As a result, the strength and hardness of the material are significantly reduced (Khalilulah et al., 2024). GTAW joints in Aluminium 6061-T6 exhibit an ultimate tensile strength ranging from 80.9 MPa to 86.7 MPa, indicating substantial softening compared with the base metal (Fakhri et al., 2022; Guzmán et al., 2019).

To restore the material properties degraded by welding, Post-Weld Heat Treatment (PWHT) can be applied. This post-weld heat treatment aims to relieve residual stresses, improve microstructural homogeneity, and restore the distribution of strengthening precipitates, thereby enhancing the strength and hardness of the material (Pratikno et al., 2020). Without PWHT, microstructural changes in the Heat-Affected Zone (HAZ) may lead to a reduction in strength and even premature material failure during service (Achmad et al., 2026; H. Wang et al., 2020). Several previous studies have investigated the effects of welding and PWHT on aluminium alloys. The microstructural characteristics and hardness distribution have been shown to significantly influence the performance of GTAW joints in Aluminium 6061-T6 (Soundararajan et al., 2022). In addition, PWHT has been reported to improve microstructural homogeneity and the mechanical properties of welded Al–Mg–Si alloy joints (Bagheri Vanani et al., 2025; Bi et al., 2024; El-Fahhar et al., 2024; Schenk et al., 2025; Yang & Chen, 2024). Nevertheless, most previous studies have been conducted using standard laboratory plate specimens, and only limited attention has been given to the application of PWHT to actual repaired components, such as Aluminium 6061-T6 calliper brackets.

Based on these considerations, further research is required to evaluate the effectiveness of Post-Weld Heat Treatment (PWHT) on repaired Aluminium 6061-T6 calliper brackets welded using the Gas Tungsten Arc Welding (GTAW) process. The evaluation was carried out through liquid penetrant testing in accordance with ASTM E165 to identify surface defects in the welded joints and Micro Vickers hardness testing based on ASTM E384 to analyse changes in the mechanical properties within the Fusion Zone (FZ), Heat-Affected Zone (HAZ), and Base Metal (BM). The findings of this study are expected to provide scientific evidence regarding the effect of PWHT on the quality of GTAW welded joints and to serve as a valuable reference for the repair of braking system components manufactured from Aluminium 6061-T6.

2. Material and methods

This study employed an experimental research design with a quantitative approach. The research object was an Aluminium 6061-T6 calliper bracket obtained from a previously used motorcycle. The material was first identified using a Thermo Fisher Quattro S Field Emission Scanning Electron Microscope equipped with Energy-Dispersive Spectroscopy (FESEM-EDS). Elemental analysis was conducted at nine measurement points and revealed an average aluminium content of 97.28 wt%, while the contents

of Mg, Si, Fe, Cr, and other alloying elements were within the specification range for Aluminium 6061. Based on these results, the material was confirmed to be Aluminium 6061 and was considered suitable for use in this study.

2.1 Specimen preparation

Artificial damage simulating field-induced cracks was introduced at the centre of the Calliper bracket, which represents the critical load-bearing region. Joint preparation was performed by machining a V-groove with a 60° included angle using a hand grinder. After the cutting process was completed, the groove was prepared in the welding area using the same hand-grinding process. The groove preparation provided sufficient space for the filler metal, thereby ensuring adequate weld penetration and producing a high-quality welded joint, as shown in Figure 1.

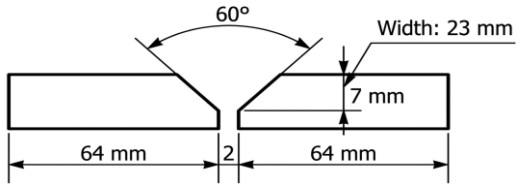

Figure 1. 60° V-Groove Preparation

Before welding, the material surface was cleaned using a liquid cleaning agent to remove contaminants that could affect the quality of the welded joint. A total of six welded specimens were prepared in this study, consisting of three specimens without PWHT and three specimens subjected to PWHT.

2.2 GTAW welding process

The welding process was carried out using an AOTAI ATIG210PAC welding machine with identical welding parameters for all specimens. The welding current was set at 180 A, the arc voltage at 18 V, the argon shielding gas flow rate at 10 L/min, and the welding speed at 100 mm/min. Alternating current (AC) was employed to provide the cathodic cleaning effect required to remove the stable aluminium oxide layer, which is difficult to break down during welding. An ER4043 filler metal with a diameter of 2.4 mm was used because of its low susceptibility to cracking and its compatibility with the Aluminium 6061 base alloy. All welding procedures were performed under the supervision of a certified welding instructor to ensure procedural consistency and uniform weld quality among the specimens. The welding parameters are summarized in Table 1.

Table 1. GTAW welding parameters for the Calliper Bracket specimens

Parameter	Value
Welding current	180 Ampere
Arc voltage	18 Volt
Shielding gas flow rate	10 L/min
Welding speed	100 mm/min
Shielding gas	Argon
Current type	AC
Filler metal	ER 4043 2,4 mm

Welding was performed on the prepared V-groove specimens to produce the welded joints used as the research specimens. After welding, the specimens were allowed to cool naturally in ambient air until

they reached approximately room temperature. Once cooled, the specimens were cleaned using a cleaning agent to remove dirt and oil residues from the welded surfaces. The GTAW process applied to the Aluminium 6061-T6 calliper bracket specimens is shown in Figure 2.

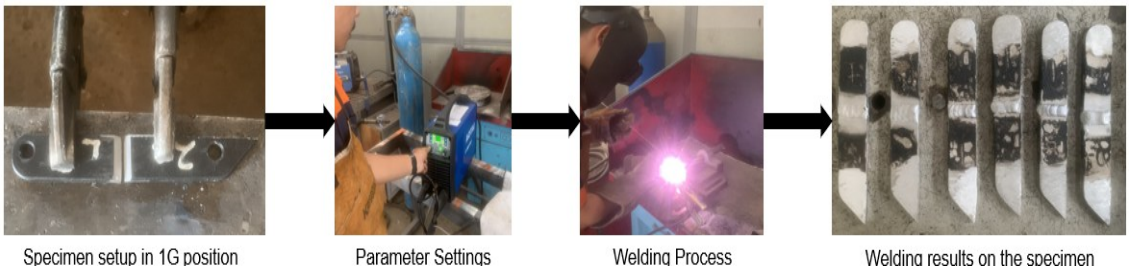

Figure 2. GTAW welding process of the Aluminium 6061-T6 Calliper Bracket specimen

2.3 Post-Weld Heat Treatment (PWHT) process

Post-Weld Heat Treatment (PWHT) was applied to selected GTAW-welded specimens to restore the material properties altered by the thermal cycle of the welding process. The PWHT parameters were established in accordance with ASTM B918, as summarized in Table 2.

Table 2. PWHT temperature parameters for the welded specimens

Process Stage	Temperature	Duration
Solution heat treatment	535 °C	Heating: 10 °C/min; Hold: 1 h
Quenching	Water (maximum 43 °C)	Until near ambient temperature
Artificial aging	175 °C	Heating: 10 °C/min; Hold: 8 h

The PWHT process was carried out using a Nabertherm muffle furnace and consisted of three sequential stages. The first stage was solution heat treatment performed at 535 °C with a heating rate of 10 °C/min from room temperature, followed by a holding time of 1 h at the target temperature, as shown in Figure 3.

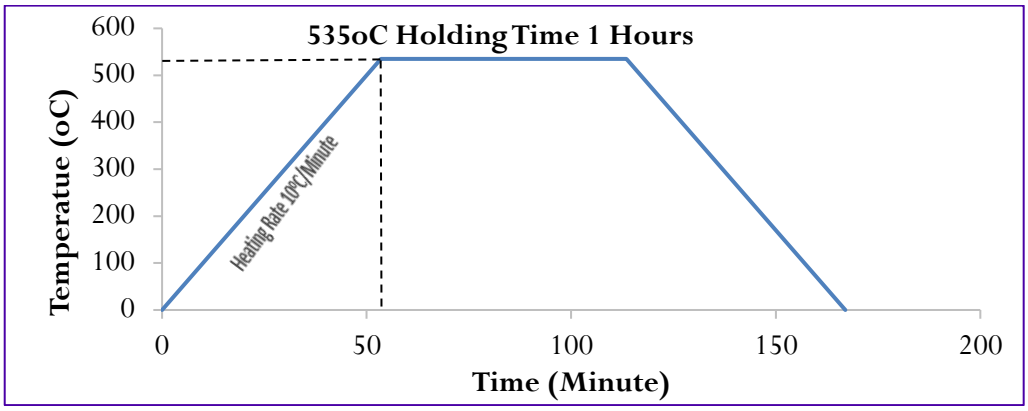

Figure 3. Temperature profile of the solution heat treatment process

After the solution heat treatment, the specimens were immediately removed from the furnace and subjected to water quenching using water maintained at a maximum temperature of 43 °C. The transfer time from the furnace to the quenching medium was kept below 10 s to ensure effective cooling. The final stage was artificial aging performed at 175 °C for 8 h with a heating rate of 10

°C/min, followed by air cooling for 10 h until the specimens reached room temperature. Meanwhile, the specimens in the non-PWHT group were maintained at room temperature throughout the treatment period. The temperature profile of the artificial aging process is shown in Figure 4.

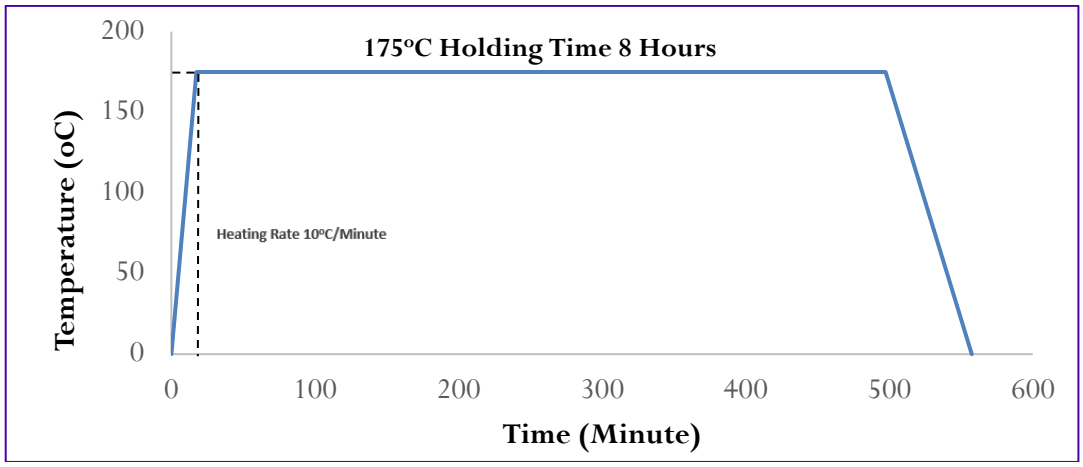

Figure 4. Temperature profile of the artificial aging process

2.4 Liquid penetrant testing

Surface discontinuities were examined on the GTAW-welded specimens before and after PWHT using the visible liquid penetrant testing method with a solvent-removable penetrant from the Magnaflux Spotcheck kit, in accordance with ASTM E165. Prior to testing, the specimen surfaces were cleaned with a solvent cleaner for 15 min to remove dirt, oil, and other contaminants. The specimens were then grouped and labelled according to their treatment condition (before and after PWHT). Subsequently, the penetrant was applied by spraying and allowed to dwell for 10 min to enable penetration into surface-opening discontinuities. After the dwell time, the excess penetrant was carefully removed using a clean cloth moistened with solvent cleaner to avoid removing the penetrant trapped within the discontinuities. A developer was then applied and allowed to develop for 10 min to reveal defect indications. The developer application process is shown in Figure 5.

Figure 5. Liquid penetrant testing procedure for the welded specimens

The inspection was performed by visual examination with the naked eye, and all defect indications were photographically documented. The test results were classified according to the defect location (face or root), defect type, and the number of indications observed on each specimen. The results were subsequently evaluated based on the acceptance criteria specified in AWS D1.2.

2.5 Micro Vickers hardness testing

Micro Vickers hardness testing was performed on the cross-section of the welded joints prepared through standard metallographic procedures using an FM-800 Micro Vickers Hardness Tester, in

accordance with ASTM E384. The test specimens, measuring 80 mm × 6 mm × 6 mm, were prepared by sequential grinding with abrasive papers ranging from 180 to 2000 grit to obtain a flat and smooth surface. Hardness measurements were conducted in three regions of the welded joint: the Fusion Zone (FZ), the Heat-Affected Zone (HAZ), and the Base Metal (BM). In the FZ, three indentations were made along the centreline of the weld metal. In the HAZ, three measurements were performed on both the left and right sides, while three measurements were also taken on both sides of the BM. The spacing between adjacent indentations was maintained at a minimum of 5 mm to prevent overlapping deformation zones caused by the indenter load. The specimen preparation and Micro Vickers hardness testing procedures are illustrated in Figure 6.

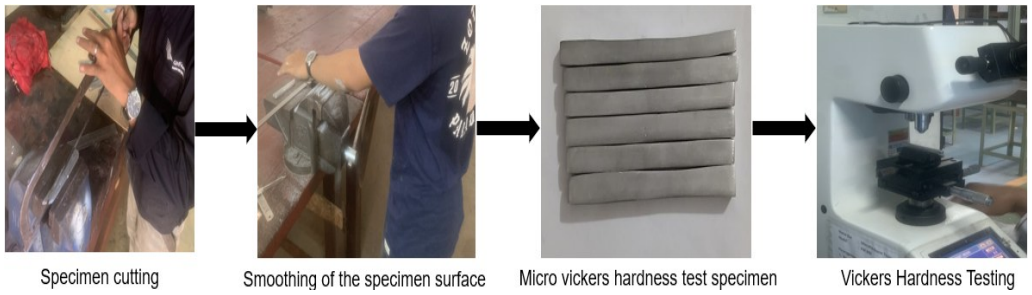

Figure 6. Specimen preparation and Micro Vickers hardness testing procedure

The hardness values were recorded directly in Vickers hardness (HV) units, and the average hardness was calculated for each region of every specimen. Subsequently, the mean hardness values obtained from the three specimens in each treatment group were used as the basis for comparative analysis of the Micro Vickers hardness.

3. Results and discussion

3.1 Liquid penetrant test results

The liquid penetrant test results revealed clear and significant differences in the characteristics of surface discontinuities between the specimens before and after PWHT. The detailed inspection results for all specimens are presented in Table 3 and Table 4.

Table 3. Liquid penetrant test results for the specimens before PWHT

Specimen	Surface	Defect type	Number of indications
1	Face	Porosity	3
		Lack of fusion	2
	Root	Porosity	3
		Lack of penetration	2
2	Face	Porosity	8
		Lack of fusion	1
	Root	Porosity	6
		Lack of penetration	1
3	Face	Porosity	3
		Lack of fusion	2
	Root	Porosity	4
Total			35

Table 4. Liquid penetrant test results for the specimens after PWHT

Specimen	Surface	Defect type	Number of indications
1	Face	Porosity	4
	Root	Porosity	5
2	Face	Porosity	2
		Lack of fusion	1
	Root	Porosity	2
3	Face	Porosity	3
	Root	Porosity	2
Total			19

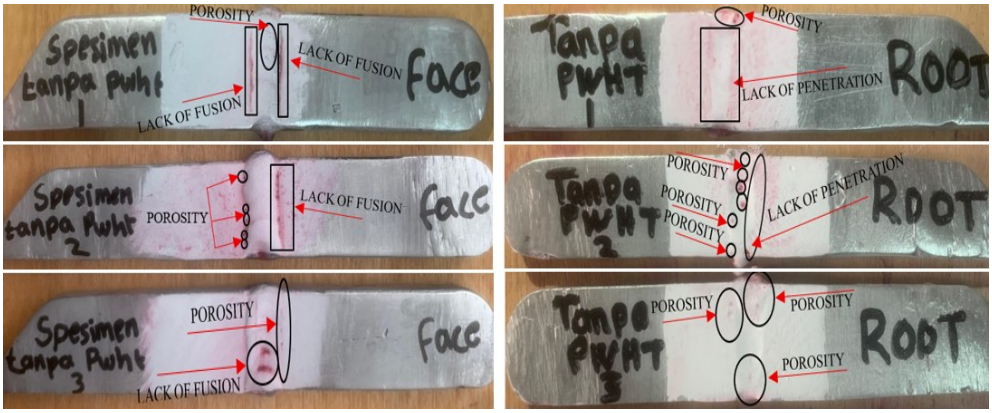

(a) (b)

Figure 12. liquid penetrant test results for the specimens before PWHT: (a) Face surface and (b) Root

The specimens in the non-PWHT group exhibited various types of surface discontinuities across all three tested specimens. As shown in Figure 12 and Table 3, Specimen 1 exhibited the most severe defects, characterized by two macroscopic linear lack-of-fusion indications extending parallel to the fusion line on the face surface, accompanied by three microscopic porosity indications. On the root surface of the same specimen, two lack-of-penetration indications were observed as irregular and discontinuous red linear indications, together with three linearly aligned porosity indications. Specimen 2 exhibited the highest number of porosity indications, with eight circular indications distributed across the weld surface, whereas Specimen 3 showed a moderate defect distribution consisting of nine indications of porosity and lack of fusion.

The presence of lack-of-fusion indications suggests that the heat input applied during the welding process was insufficient to achieve complete metallurgical bonding between the ER4043 filler metal and the Aluminium 6061-T6 base metal at the fusion boundary. This condition resulted in planar discontinuities that may act as stress concentration sites when the welded joint is subjected to tensile or cyclic loading. Meanwhile, the lack-of-penetration indications observed on the root surface indicate that the molten metal failed to penetrate completely to the root of the V-groove, leaving unbonded regions that may serve as potential crack initiation sites. Porosity in aluminium welds is primarily caused by the evolution of dissolved hydrogen during solidification. In the molten state, aluminium has a significantly higher hydrogen solubility than in the solid state. As the weld metal solidifies rapidly, the dissolved hydrogen has insufficient time to escape from the weld pool and becomes trapped within the solidifying weld metal, forming numerous small voids that appear as porosity.

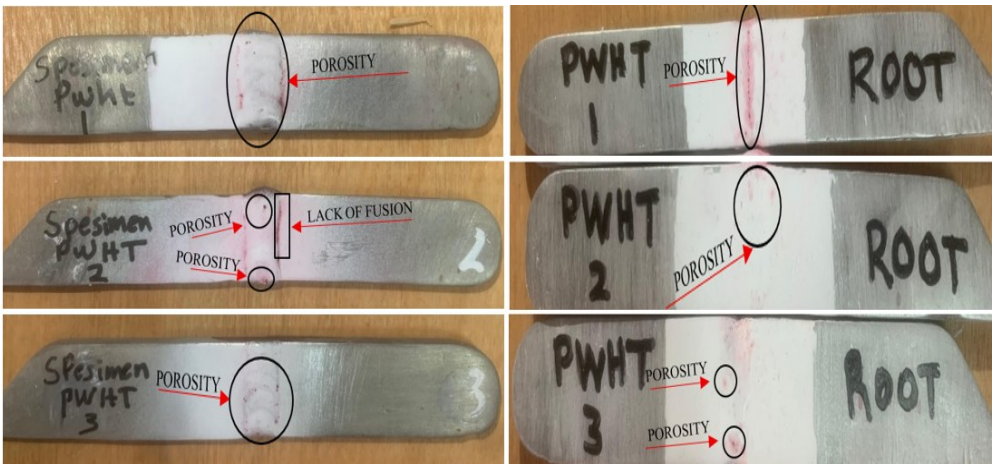

(a) (b)

Figure 13. Liquid penetrant test results for the specimens after PWHT: (a) Face surface and (b) Root

Following PWHT, the liquid penetrant test results demonstrated a significant improvement in the surface integrity of the welded joints, as shown in Figure 13 and summarized in Table 4. Critical linear discontinuities, such as lack-of-fusion and lack-of-penetration indications, were no longer observed in any of the specimens, except for a single microscopic lack-of-fusion indication on the face surface of PWHT Specimen 2. This indication appeared as a thin, faint, and discontinuous red line, in contrast to the dense and continuous indications observed before PWHT. The remaining discontinuities after PWHT consisted only of scattered microscopic porosity indications, ranging from 2 to 5 indications on each specimen surface. This number was substantially lower than that observed before PWHT, indicating that the post-weld heat treatment contributed to improving the quality and homogeneity of the welded joints.

The improvement observed in the liquid penetrant test results after PWHT should be interpreted from a metallurgical perspective. PWHT does not physically fill or eliminate pre-existing welding defects, such as porosity or lack-of-fusion regions. The voids and imperfections formed during weld metal solidification remain structurally present after the heat treatment process. The reduction in the number and intensity of the penetrant indications is primarily attributed to two mechanisms. First, during the solution heat treatment stage, the aluminium alloy undergoes significant thermal expansion, which can partially reduce the opening of narrow planar discontinuities. As a result, the ability of these discontinuities to retain and accumulate the penetrant is diminished. Second, the relaxation of welding-induced residual stresses during PWHT reduces the driving force responsible for keeping microcrack tips open. Consequently, the penetrant trapped within the discontinuities is less likely to bleed back to the surface, resulting in weaker and less distinct indications. The combined effect of these mechanisms explains why the PWHT-treated specimens consistently exhibited fewer defect indications and no longer showed macroscopic linear indications, even though the geometric discontinuities formed during welding may still remain beneath the surface.

According to the AWS D1.2 Structural Welding Code—Aluminium, linear indications such as lack of fusion and lack of penetration are classified as critical discontinuities. Therefore, Specimen 1 and Specimen 2 in the non-PWHT group were considered unacceptable based on the AWS D1.2 visual acceptance criteria, as the size and characteristics of the observed linear indications exceeded the maximum allowable limit of 3 mm. In contrast, Specimen 3 in the non-PWHT group and all specimens in the PWHT group were considered acceptable because the remaining defect indications were within the acceptance limits specified by AWS D1.2.

3.2 Micro Vickers hardness test results

Micro Vickers hardness testing was performed in the Fusion Zone (FZ), Heat-Affected Zone (HAZ), and Base Metal (BM) of all six welded specimens. In addition, three hardness measurements were obtained from the raw-material calliper bracket, yielding values of 101.1 HV, 97.0 HV, and 113.8 HV, with an overall average hardness of 103.96 HV. These values are consistent with the characteristics of precipitation-hardened Aluminium 6061-T6, in which Mg_2Si precipitates act as effective barriers to dislocation motion. The presence of these precipitates increases the material's resistance to plastic deformation, resulting in the relatively high hardness characteristic of the T6 temper condition.

Table 5. Average Micro Vickers Hardness Values (HV) of the Specimens before and after PWHT

Group	Specimen	FZ (HV)	HAZ (HV)	BM (HV)
After PWHT	1	103	107.4	92.93
	2	80.86	87.4	95.96
	3	92.93	98.56	98.23
	Average	92.26	97.78	95.70
Before PWHT	1	87.26	60.13	61.86
	2	54.33	65.93	57.53
	3	60.43	82.93	67.93
	Average	67.34	69.66	62.44

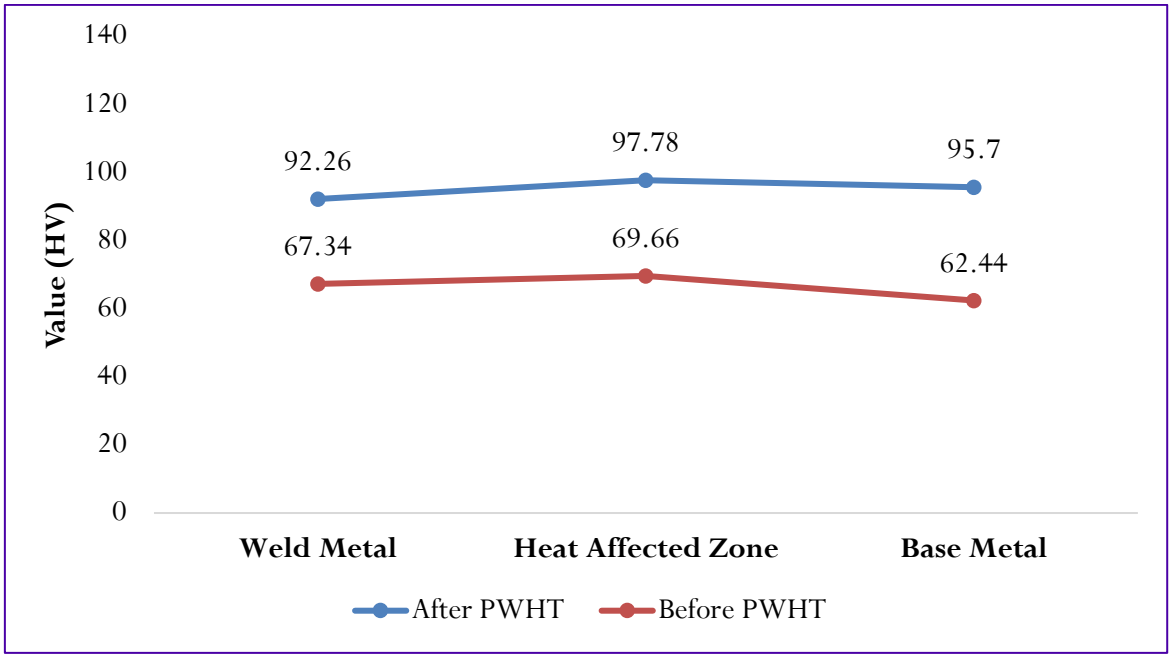

Figure 14. Average Micro Vickers Hardness Values (HV) of the Specimens Before and After PWHT

The hardness data presented in Table 5 and Figure 14 demonstrate a consistent and significant reduction in micro-Vickers hardness across all three weld regions after repair by the GTAW process compared with the raw material. Before PWHT, the average hardness in the Fusion Zone (FZ) was 67.34 HV, representing a 35.2% decrease from the average hardness of the raw material (103.96 HV). In the Heat-Affected Zone (HAZ), the average hardness decreased by 32.9% to 69.66 HV, whereas the greatest reduction was observed in the Base Metal (BM), where the average hardness decreased by

39.9% to 62.44 HV. Overall, the average hardness across all weld regions decreased by approximately 36% relative to the initial material condition.

The observed reduction in hardness is consistent with the dissolution and coarsening of Mg_2Si precipitates caused by the high temperatures generated during the GTAW thermal cycle. In the Fusion Zone (FZ), the material underwent complete melting followed by resolidification without controlled cooling, resulting in a relatively coarse dendritic microstructure with limited precipitation strengthening. Consequently, the material exhibited a reduced resistance to plastic deformation, leading to lower hardness values. In the Heat-Affected Zone (HAZ), the temperature was sufficiently high to dissolve the previously formed fine precipitates and promote grain-boundary liquation without causing complete melting. As a result, a softened region with a reduced population of strengthening precipitates was formed, leading to a decrease in hardness. Meanwhile, although the Base Metal (BM) was located farthest from the heat source, it was still exposed to sufficient thermal energy to induce partial over-aging and the coarsening of Mg_2Si precipitates. This explains why a substantial reduction in hardness was also observed in the BM, despite the absence of melting and the less severe thermal exposure compared with the FZ and HAZ.

Following PWHT, all three weld regions exhibited a significant increase in hardness. The average hardness in the Fusion Zone (FZ) increased from 67.34 HV to 92.26 HV, corresponding to an increase of 36.99% and recovering to 88.75% of the raw material hardness. In the Heat-Affected Zone (HAZ), the average hardness increased to 97.78 HV, representing a 40.37% improvement over the pre-PWHT condition and reaching 94.06% of the raw material hardness. Meanwhile, the Base Metal (BM) exhibited the greatest relative improvement, with the average hardness increasing from 62.44 HV to 95.70 HV, corresponding to an increase of 53.27%. This value is equivalent to 92.06% of the raw material hardness. Overall, the average hardness recovery across the three weld regions reached 91.62% of the raw material hardness after PWHT.

The improvement in hardness is attributed to the re-precipitation of fine Mg_2Si precipitates during the artificial aging stage of the PWHT process. These newly formed precipitates act as effective barriers to dislocation motion, thereby increasing the material's resistance to plastic deformation. This mechanism, known as precipitation strengthening, is the primary strengthening mechanism responsible for the improvement in mechanical properties and the recovery of hardness in Aluminium 6061-T6 following post-weld heat treatment. The percentage increase in hardness from the pre-PWHT to the post-PWHT condition for each weld region is summarized in Table 6.

Table 6. Average Micro Vickers Hardness Values and Hardness Improvement Percentages

Region	Raw Material (HV)	Before PWHT (HV)	After PWHT (HV)	Hardness Improvement / Recovery (%)
FZ	103.96	67.34	92.26	36.99% / 88.75%
HAZ		69.66	97.78	40.37% / 94.06%
BM		62.44	95.70	53.27% / 92.06%
Average	103.96	66.48	95.25	43.28% / 91.62%

The findings of this study are in strong agreement with those reported in previous studies. Post-Weld Heat Treatment (PWHT) applied to Al–Mg–Si alloys welded using the oscillating laser welding process has been shown to significantly improve the homogeneity of precipitate distribution in the weld metal and the Heat-Affected Zone (HAZ), resulting in measurable hardness recovery (Yang & Chen, 2024). The HAZ is the region most susceptible to softening following GTAW of Aluminium 6061-T6 because of the dissolution and coarsening of strengthening precipitates (Soundararajan et al., 2022). However,

this softening can be substantially reversed through the application of an appropriate post-weld heat treatment that restores the T6 temper condition.

The hardness distribution pattern observed in this study, in which the Heat-Affected Zone (HAZ) exhibited the highest absolute hardness after PWHT compared with the Fusion Zone (FZ) and the Base Metal (BM), is likely associated with differences in the concentration of dissolved alloying elements and the precipitate distribution in each region following the re-aging process. This finding is consistent with the microstructural observations reported in previous studies. In Aluminium 6061 welded by the fiber laser welding process, post-heat-treatment microstructural variations have been shown to produce different levels of hardness recovery across the various weld regions (He et al., 2025).

Another noteworthy finding is that the Base Metal (BM), although located farthest from the weld pool, exhibited the lowest hardness before PWHT while also showing the greatest relative increase in hardness after PWHT. This behaviour can be attributed to the occurrence of partial over-aging in the BM during the welding process, where exposure to moderate thermal cycles caused the pre-existing fine precipitates to coarsen and lose their coherency with the aluminium matrix. During the solution heat treatment stage of PWHT, these coarsened precipitates were effectively re-dissolved into the matrix. Subsequently, the artificial aging stage promoted the re-precipitation of a finer and more uniformly distributed population of strengthening precipitates, which acted as effective barriers to dislocation motion. Consequently, hardness recovery in the BM was more efficient than in the other weld regions relative to its over-aged condition prior to PWHT, resulting in the highest percentage increase in hardness following post-weld heat treatment.

4. Conclusion

This study evaluated the effect of Post-Weld Heat Treatment (PWHT) on surface discontinuity characteristics and Micro Vickers hardness distribution in GTAW-repaired Aluminium 6061-T6 calliper brackets. The liquid penetrant test results showed that the specimens before PWHT exhibited a total of 35 defect indications identified across six specimen surfaces, consisting of macroscopic linear lack-of-fusion and lack-of-penetration indications, together with multiple porosity indications. Based on the AWS D1.2 acceptance criteria, two of the three specimens in the non-PWHT group were classified as unacceptable. After PWHT, the total number of defect indications decreased to 19, all of which consisted of scattered microscopic porosity indications. All specimens in the PWHT group satisfied the AWS D1.2 acceptance criteria. The reduction in the severity of the detected indications is attributed to thermal stress relaxation and matrix expansion during PWHT, which reduced the opening of defect boundaries. Therefore, the reduction in the number of detectable indications should not be interpreted as the physical elimination of geometric discontinuities, but rather as a consequence of material changes that reduced the ability of the discontinuities to retain and release penetrant to the surface during inspection.

The Micro Vickers hardness test results showed that the GTAW repair process reduced the average hardness in all weld regions by approximately 36% compared with the raw material hardness of 103.96 HV. Before PWHT, the average hardness values were 67.34 HV in the Fusion Zone (FZ), 69.66 HV in the Heat-Affected Zone (HAZ), and 62.44 HV in the Base Metal (BM). After PWHT, the hardness increased to 92.26 HV in the FZ, 97.78 HV in the HAZ, and 95.70 HV in the BM. These values correspond to hardness increases of 37.01%, 40.40%, and 53.27%, respectively, with an overall hardness recovery of 91.62% relative to the raw material condition. This recovery resulted from the re-precipitation of fine, coherent Mg_2Si precipitates during the artificial aging stage, which restored the precipitation-strengthening mechanism previously disrupted by the welding thermal cycle.

Overall, the findings confirm that PWHT is an effective post-weld treatment for GTAW repair of Aluminium 6061-T6 calliper brackets because it significantly improves both the surface integrity and the mechanical hardness of the welded joints. The application of PWHT effectively reduced the severity of surface discontinuities while restoring the hardness degraded by the welding thermal cycle. Therefore, the combination of GTAW repair welding and PWHT designed to restore the T6 temper condition can be considered a technically feasible and economically practical strategy for recovering the structural performance of damaged calliper brackets. This approach enables damaged components to be repaired and returned to service with mechanical properties approaching those of the original material.

Author's declaration

Author contribution

Dipo Ariyo Nugroho: Conceptualization, experimental design, specimen preparation, experimental investigation, data collection, and writing-original draft. **Zainal Abadi:** Conceptualization, methodology, validation, writing-review and editing, and supervision. **Rifelino:** Validation, writing-review and editing, and supervision. **Andril Arafat:** Validation, writing-review and editing, and supervision.

Funding statement

This research received no specific grant from any funding agency in the public, commercial, or not-for-profit sectors.

Data availability

The raw data supporting the findings of this study are available from the corresponding author upon reasonable request.

Acknowledgements

The authors would like to express their sincere gratitude to the lecturers of the Department of Mechanical Engineering, Faculty of Engineering, Universitas Negeri Padang, for their guidance and support throughout this study.

Conflict of interest

The authors declare that they have no financial or non-financial conflicts of interest related to the subject matter or materials discussed in this manuscript.

Ethical clearance

Not applicable.

AI statements

The translation of this manuscript was assisted by ChatGPT, while Grammarly was used for grammar checking and language refinement to improve the readability and linguistic quality of the manuscript. The authors independently reviewed the accuracy, correctness, and contextual appropriateness of all

AI-assisted outputs to ensure consistency with the topic and scope of this study. No AI-generated sentences, tables, or figures were incorporated directly into this manuscript. The authors take full responsibility for the entire content of this manuscript.

Publisher's and Journal's Note

Researcher and Lecturer Society as the publisher, and the editor of Journal of Engineering Researcher and Lecturer state that there is no conflict of interest towards this article publication.

References

Achmad, Z., Ismail, A. E. bin, Seputro, H., & Marliana, E. (2026). The effect of T6 heat treatment on the tensile, impact, and fatigue properties of Al6061-fly ash composites. *Teknomekanik*, *9*(2), 162–176. https://doi.org/10.24036/teknomekanik.v9i2.50672

Bagheri Vanani, B., Mehraban Dehaqani, M. R., Abbasi, M., Sadeqi Bajestani, M., Mohammadkhah, M., & Klinge, S. (2025). Effects of PWHT on the microstructure, corrosion, tribology, and mechanical properties of mild steel welds under different joining positions: Experimental and Numerical Study. *Journal of Materials Research and Technology*, *38*, 752–767. https://doi.org/10.1016/j.jmrt.2025.07.253

Bi, J., Chi, J., Song, H., Shao, H., Wang, K., Yang, Z., Jia, X., & Dong, G. (2024). Enhancing tensile properties of MIG welded AA6061 joints: Effect of pulse mode and post-weld heat treatment. *Materials Today Communications*, *39*, 109156. https://doi.org/10.1016/j.mtcomm.2024.109156

Carvalho, G. H. S. F. L., Campatelli, G., Cota, B. S., Campanella, D., & Di Lorenzo, R. (2024). Development of a NC-Controlled GTAW-Based Wire Arc Additive Manufacturing System for Using Friction Stir Extrusion Recycled Wires. *Machines*, *13*(1), 10. https://doi.org/10.3390/machines13010010

Cheng, J., Song, G., Zhang, X., Liu, C., & Liu, L. (2021). Review of Techniques for Improvement of Softening Behavior of Age-Hardening Aluminum Alloy Welded Joints. *Materials*, *14*(19), 5804. https://doi.org/10.3390/ma14195804

Croccolo, D., De Agostinis, M., Olmi, G., & Tizzanini, A. (2013). Analysis of the Stress State in Brake Caliper Mounts of Front Motorbike Suspensions. *Advances in Mechanical Engineering*, *5*. https://doi.org/10.1155/2013/525010

El-Fahhar, H. H., Gadallah, E. A., Habba, M. I. A., Seleman, M. M. E.-S., Ahmed, M. M. Z., Mohamed, A. Y., & Fouad, R. A. (2024). Effect of post-weld heat-treatment and solid-state thermomechanical treatment on the properties of the AA6082 MIG welded joints. *Scientific Reports*, *14*(1), 4380. https://doi.org/10.1038/s41598-024-53795-6

Fakhri, A. A., Basyirun, B., & Fikrie, A. (2022). Analysis of tensile strength and microstructure on GTAW- Aluminum 6061 welding results. *Journal of Engineering and Applied Technology*, *3*(2), 94–100. https://doi.org/10.21831/jeatech.v3i2.53149

Guzmán, I., Granda, E., Acevedo, J., Martínez, A., Dávila, Y., & Velázquez, R. (2019). Comparative in Mechanical Behavior of 6061 Aluminum Alloy Welded by Pulsed GMAW with Different Filler Metals and Heat Treatments. *Materials*, *12*(24), 4157. https://doi.org/10.3390/ma12244157

He, B., Chen, G., Zheng, J., & Huang, P. (2025). Investigation of Weld Formation, Microstructure and Mechanical Properties of Small Core Diameter Single Mode Fiber Laser Welding of Medium Thick 6061 Aluminum Alloy. *Photonics*, *12*(12). https://doi.org/10.3390/photonics12121204

Khalilulah, I., Gunawan, I., & Siswanto, A. (2024). Analysis Of The Effect Of Electric Current In TIG Welding Process On The Strength Of Welded Joints Of Aluminium 6061 Metal Material. *Jurnal Vokasi Mekanika (VoMek)*, *6*(4), 405–419. https://doi.org/10.24036/vomek.v6i4.831

Kumar, M., Baloch, M. M., Abro, M. I., Memon, S. A., & Chandio, A. D. (2019). Effect of Artificial Aging Temperature on Mechanical Properties of 6061 Aluminum Alloy. *Mehran University*

Research Journal of Engineering and Technology, *38*(1), 31–36. https://doi.org/10.22581/muet1982.1901.03

Liu, Y., Wang, S., Shi, S., & Tan, J. (2026). Finite Element Analysis and Optimization of Automotive Disk Brakes Using ANSYS. *Symmetry*, *18*(2), 349. https://doi.org/10.3390/sym18020349

Pratikno, H., Rachmatullah, T., & Ikhwani, H. (2020). Influence of Pre-Weld Heat Treatment and Aging Post-Weld Heat Treatment on Tensile Test and Microstructure of Aluminium 6061 Weld Joint. *International Journal of Offshore and Coastal Engineeing*, *4*(1), 1. https://doi.org/10.12962/j2580-0914.v4i1.8701

Rajakumar, S., Muralidharan, C., & Balasubramanian, V. (2011). Predicting tensile strength, hardness and corrosion rate of friction stir welded AA6061-T6 aluminium alloy joints. *Materials & Design*, *32*(5), 2878–2890. https://doi.org/10.1016/j.matdes.2010.12.025

Schenk, J., Hoefer, K., & Hensel, J. (2025). Process and joint properties of GMA welded alloy AW6082 with TiB2-modified filler material. *Welding in the World*, *69*(12), 3823–3836. https://doi.org/10.1007/s40194-025-02157-5

Shukla, P., & Choudhary, D. (2022). Experimental investigation of wear failure of sliding joint of guide pin and bracket of four wheeler disc brake assembly. *International Journal of Vehicle Noise and Vibration*, *18*(3/4), 186. https://doi.org/10.1504/IJVNV.2022.128278

Soundararajan, R., Ramkumar, K. R., Sivasankaran, S., & Kim, H. S. (2022). Enhancement of tensile strength in AA 6061-T6 plates joined by gas tungsten arc welding using high entropy alloy filler sheet. *Materials Science and Engineering: A*, *832*, 142481. https://doi.org/10.1016/j.msea.2021.142481

Stewart, M. (2021). Fabrication, welding, and in-shop inspection. In *Surface Production Operations* (pp. 197–284). Elsevier. https://doi.org/10.1016/B978-0-12-803722-5.00006-9

Wang, H., Liu, X., & Liu, L. (2020). Research on Laser-TIG Hybrid Welding of 6061-T6 Aluminum Alloys Joint and Post Heat Treatment. *Metals*, *10*(1), 130. https://doi.org/10.3390/met10010130

Wang, Z., Fan, X., Zhang, Z., Song, G., & Liu, L. (2024). Microstructure and mechanical properties of 7075-T6 aluminum alloy plates by welding with weld reinforcement rolling. *Materials Science and Engineering: A*, *889*, 145854. https://doi.org/10.1016/j.msea.2023.145854

Wang, Z., Zhang, Z., Lang, Q., Song, G., & Liu, L. (2023). Microstructure evolution and deformation behavior of TIG welded 7075-T6 aluminum alloy followed by partial hot rolling. *Journal of Manufacturing Processes*, *94*, 524–538. https://doi.org/10.1016/j.jmapro.2023.04.006

Yang, L., & Chen, X. (2024). Effect of post-weld heat treatment methods on microstructure and fatigue behavior of Al-Mg-Si alloy oscillating laser welding. *Materials Today Communications*, *39*, 109078. https://doi.org/10.1016/j.mtcomm.2024.109078